Applied Water Science (2024) 14:225
https://doi.org/10.1007/s13201-024-02292-2

ORIGINAL ARTICLE

Enhanced cadmium (Cd^{2+}) removal from wastewater using integrated inclined plate settler and composite adsorbent coating

Gilbert C. Chintokoma[1] · Yonas Chebude[1,2] · Shimelis K. Kassahun[3] · Abayneh G. Demesa[4] · Tuomas Koiranen[4]

Received: 1 April 2024 / Accepted: 9 September 2024

Abstract

Bottlenecks inherent in batch and column adsorption configurations have impeded the implementation of the adsorption technique in large-scale wastewater treatment systems. This study mainly aimed to develop an innovative wastewater treatment prototype that integrates inclined plate settlers (IPS) and composite adsorbent coating (CAC). The objective is to enable the removal of Cd^{2+} from aqueous solutions in a continuous setup, thereby enhancing its practicality for large-scale applications. The combined IPS-CAC system was optimized at various angle of inclination (θ), influent flow rate (Q) and adsorbate initial concentration (C_o) using the Box–Behnken Design (BBD) of the Response Surface Methodology (RSM). At optimized operating parameters ($\theta = 45°$, $Q = 5$ ml/min and $C_i = 1.87$ mg/L) the IPS-CAC Cd^{2+} predicted ($R^2 = 0.9926$) and experimental removal efficiencies were 75.8% and $69.7 \pm 4.67\%$, respectively. The IPS-CAC breakthrough adsorption capacity was 9.6 mg/g. Comparing IPS-CAC performance with a tank without plates and IPS with plain plates, the Cd^{2+} removal efficiencies were $2.4 \pm 0.1\%$ and $4.6 \pm 1.1\%$, respectively, confirming the synergistic effect of IPS and CAC. Additionally, breakthrough curves were acquired for various flow rates, cadmium influent concentrations, and plate inclination angles. Only a 10% decline in the removal effectiveness (from 69.7 to 59.7%) of the CAC after three adsorption–regeneration cycles was observed, indicating its stability for heavy metal removal. The results underpin the potential of using IPS-CAC for industrial wastewater treatment and enhancing the use of adsorption on a larger scale.

Keywords Breakthrough curve · Inclination angle · Composite adsorbent coating · Inclined plate settler · Optimization · Synergistic integration

Introduction

The discharge of substantial quantities of valuable heavy metals, including cadmium into global wastewater systems remains a pressing industrial concern. In industrial waste, cadmium can be found as a natural deposit, but it is exceedingly hazardous as it tends to accumulate in the environment (Gupta et al. 2021). Cadmium serves as a key constituent in various industrial sectors, including plating, battery manufacturing (specifically for cadmium–nickel batteries), phosphate-based fertilizer manufacture, stabilizer formulation, and alloy development (Demim et al. 2013). According to Genchi et al. (2020) exposure to cadmium occurs through a number of pathways including inhalation, smoking and consumption of contaminated water and food. These exposures have been linked to the development of chronic renal failure, cancer, as well as bone demineralization and fragility in both human and animal populations (Mahdi et al. 2021). Moreover, cadmium exposure has been associated with several symptoms, including vitamin D deficiency, respiratory-related ailments, and gastrointestinal disorders that result in loss of red blood cells. These conditions can impede the proper functioning of calcium in both human and animal bodies (Filipič, 2012; Genchi et al. 2020). It is

✉ Gilbert C. Chintokoma
chintokomagc@gmail.com

1 African Centre of Excellence for Water Management, College of Natural and Computational Sciences, Addis Ababa University, P.O. Box 1176, Addis Ababa, Ethiopia

2 Department of Chemistry, College of Natural and Computational Sciences, Addis Ababa University, P.O. Box 1176, Addis Ababa, Ethiopia

3 School of Chemical and Bio Engineering, Addis Ababa University, P.O. Box 1176, Addis Ababa, Ethiopia

4 Department of Separation Science, School of Engineering Science, LUT University, Skinnarilankatu 34, 53850 Lappeenranta, Finland

Published online: 19 September 2024

therefore imperative to eliminate cadmium from industrial effluent prior to their introduction into aquatic environments, as their detrimental impacts on human health have been unequivocally demonstrated. The elimination of the cadmium is pivotal for protection of human health, preserving environmental quality and supporting safe re-use of waste water. Among the available wastewater treatment techniques, adsorption is currently the most frequently utilized method for water purification, because of its high pollutant removal efficiency, simplicity and its potential to treat a large quantity of water in semi-continuous system with acceptable costs (Somma et al. 2021). Although activated carbon has numerous advantages as an adsorbent for pollutant removal, there are still certain gaps that impede its widespread use in large-scale wastewater treatment including limitations in its synthesis process, challenges in regeneration, difficulties in recyclability, and limitations in selectivity toward contaminants (Gul et al. 2022). For easy phase separation, the adsorbent material must be coated or immobilized onto a substrate or supporting material.

Among the available primary water and wastewater treatment technologies for highly turbid effluent are the inclined plate settlers (IPS). These are high rate sedimentation devices consisting of a series of inclined parallel plates forming channels (plate stack) into which turbid waters can be fed for settling (Leung and Probsteln 1983). An inclined plate settler (IPS) has a lower hydraulic retention time (HRT) compared to a standard gravity settler, due to its shorter settling distance. In this situation, the available settling area depends on the total area of the plates projected onto a horizontal surface (Hyun and Kang 2023).

The use of IPS for turbidity removal or as a pretreatment for other treatment techniques is well documented in the literature (Chintokoma et al. 2015; Clark et al. 2007a, 2007b; Dorea et al. 2014; Elligson et al. 2014; Kasenene et al. 2021; Kayhanian et al. 2001; Sarkar et al. 2007; Wisniewski 2014; Zhang et al. 2020). Recently IpS has been used in combination with other water and wastewater treatment techniques (Bo et al. 2015). For example, IPS has been used in combination with constructed wetland (Kasenene et al. 2021), electrocoagulation (Hu et al. 2022) and activated carbon sponge tubes (Hyun and Kang 2023) for turbidity and fecal coliform removal, oil removal and for the treatment of urban stormwater runoff, respectively. However, all these recent studies had the combinations of the techniques in series configurations, i.e., one treatment technique after the other in separate treatment units. The current study is unique as it aims at integrating IPS and adsorption in one treatment unit so as to decrease the treatment footprint. Hence, we postulate that the immobilization of activated carbon on inclined plate setters will considerably decrease adsorbent leaching, improve adsorbent recyclability, increase surface area for adsorbent–adsorbate contact and consequently enhance the effectiveness of pollutant (i.e., Cd^{2+}) removal. *Prosopis juliflora* is selected in this study as a precursor for preparing activated carbon because it is readily available and is considered an invasive species that is spreading rapidly in many sub-Saharan countries including Ethiopia.

To the best of the authors knowledge, there has been no prior reported work of a heavy metal removal system that integrates IPS and adsorption. By leveraging the synergistic effect of IPS and CAC, this combination may have the following benefits: (a) enhancing the removal efficiency of Cd^{2+} by the synergistic effect of IPS and CAC (which means removal of Cd^{2+} by adsorption and sedimentation) (b) reducing the footprint needed for individual adsorption apparatus and settler under the same flow rate; and (c) enhancing the potential of scaling up the system for large-scale wastewater treatment. To this end, this work was aimed at developing an innovative method for treating wastewater influent by combining the strengths of both IPS and adsorption techniques. The effects of angle of plate inclination (θ_p), influent flow rate (Q) and adsorbate initial concentration (C_i) on Cd^{2+} percent removal efficiency (%) was studied by employing the Box–Behnken Design (BBD) of the Response Surface Methodology (RSM). The adsorption capacity (mg/g) of IPS-CAC was explored by breakthrough curve analysis (BTCA). Additionally, to compare the performances, the Cd^{2+} percent removal efficiencies (%) of IPS-CAC was compared with IPS with no plates (IPS-NP) and IPS with plain plates (IPS-PP). Adsorption–desorption experiments were also conducted to assess the regeneration potential of the CAC.

Materials and methods

Chemicals and materials

All chemicals utilized in this investigation were of analytical grade and were employed without additional purification. These chemicals included zinc chloride ($ZnCl_2$), sodium hydroxide (NaOH), cadmium chloride hydrate ($CdCl_2 \cdot H_2O$), and hydrochloric acid (HCl) were purchased from Thomas Baker Chemicals, Spectrum Chemical. Acrylic Polymer Emulsion (APE) (Ecronova® RA 127) was supplied by Mallard Creek Polymer. Plexiglass (3 mm thickness) was sourced locally.

Preparation of activated carbon and composite adsorbent coating (CAC)

The *Prosopis juliflora* wood material was used as the precursor for preparing the activated carbon owing to its significant porosity, large surface area, and copious sorption capacity. The activated carbon was prepared using pyrolysis method utilizing both chemical and thermal activation (Chintokoma

et al. 2024a, b). In summary the dried biomass was impregnated with a boiling solution of zinc chloride ($ZnCl_2$) using an impregnation ratio (IMPR) (mass of $ZnCl_2$ to mass of dried *Prosopis Juliflora*) of 1:1.8 for 2 h and soaked in the same $ZnCl_2$ solution for 24 h. After 24 h, the excess zinc chloride solution was decanted off and the biomass was air-dried after thorough washing with DI water. Subsequently the material was placed in a muffle furnace, carbonized at 595 °C for 174 min to eliminate the volatile matter. The carbon was then thoroughly washed with DI water, oven dried at 40 °C for 24 h, powdered and then activated in a muffle furnace at 800 °C for a period of 120 min at 10 °C/min heating rate to develop the porosity and surface area. Finally, the powdered activated carbon (PAC) was sieved through a 150 microns (μm) mesh and stored in airtight plastic bags for characterization and subsequent CAC preparation.

In an attempt to obtain a high surface area and a stable surface for adsorption, a facile sol–gel method adapted from (Azha and Ismail 2019) was used for the CAC preparation. Activated carbon prepared from *Prosopis juliflora* wood (PJAC), Cotton Cellulosic Fiber (CCF), APE and DI water, were all used in CAC fabrication (Chintokoma et al. 2024a, b).

The synthesis of the PJAC/APE-CCF (CAC) adsorbent coating involved the blending of PJAC/APE/DI through mixing 2 ml of APE and 4 ml of DI water with 0.25 g of the activated carbon prepared from *Prosopis Juliflora* wood (PJAC) per 75cm^2 of CCF (i.e., 0.00333 g/cm^2). The resulting slurry was mixed with a magnetic agitator (Model RT Power) for approximately 3 h to form a homogeneous solution. For every 15 cm × 5 cm (75cm^2) of CCF per given adsorbent dosage, 2 ml and 4 ml of APE and deionized water were used, respectively. For instance, in case of a 0.25 g CAC, 2 ml of APE and 4 ml of DI water were used per 0.25 g of adsorbent on a 15 cm × 5 cm (75 cm^2) CCF. The amount of coating was measured gravimetrically by Eq. 1.

$$\mathbf{Wt}_{\mathrm{CAC}} = \mathbf{Wt}_{\mathrm{APJW/APE-CCF\ after\ drying}} - \mathbf{Wt}_{\mathrm{CCF\ before\ coating}} \quad (1)$$

The CCF was placed on same sized[1] Plexiglass of thickness 0.3 cm and then the slurry was applied on the CCF attached to the IPS plate on both sides using a brush. The prepared CAC-Plates were dried at 70 °C for 12 h. The dried CAC plates were stored in airtight containers for use in further IPS-adsorption tests.

[1] i.e., the CCF had the same size as the plexiglass plate while just leaving enough space, e.g., ≤ 1 cm on both ends of the plate to allow for plate insertion onto the IPS plate grooves.

Physicochemical properties analysis

The surface properties, including specific surface area and pore volume, are crucial for the performance of adsorption materials. They influence how effectively a material can capture and hold pollutants, as these properties dictate the extent of mass transfer, which involves the movement of adsorbate molecules onto the adsorbent surface. In this regard, a CAC powdered sample was prepared for both Brunauer–Emmet–Teller (BET) Surface Area (S_{BET}) and particle size distribution (PSD) analysis. This involved mixing a known amount of APE, DI water and adsorbate (adsorbate dosage) for 180 min until a homogeneously blend. Then the homogeneous mixture was subjected to drying for 7 h at 40 °C in a vacuum oven (Townson + Mercer) under 300 mbar pressure. Subsequently, the desiccated material was pulverized into a fine powder and sieved through a 150 μm mesh for S_{BET} and PSD analyses.

The pore volume (cm^3/g), surface area (m^2/g), and pore size (125.3 Å) were determined through the utilization of the N_2 adsorption/desorption isotherm technique employing the BET method. The N_2 adsorption/desorption isotherms were obtained by conducting measurements at a temperature of 77.279 K using a BET surface analyzer (Micromeritics Instrument Flex Version 6.01).

Scanning Electron Microscopy (Hitachi TM 1000) was used to analyze surface morphology of both PAC and CAC. The elemental analysis of the CAC was performed using Scanning Electron Microscopy-Energy Dispersive X-Ray Analysis (SEM–EDX) (Hitachi TM 1000).

The alteration in the CAC's functional group prior to and following adsorption was examined by FTIR spectroscopy (PerkinElmer Spectrum 65) (spectral range; 4000 cm^{-1}–400 cm^{-1}). The pH Point of Zero Charge (pH_{PZC}) was measured using a pH drift approach. In summary, 75 cm^2 (15 cm × 5 cm) of CAC coated with 0.25 g of adsorbent was each put in 10 flasks holding 80 mL of a 0.1 M NaCl solution but having ranges of pH values from 2 to 11. The pH adjustment was done using 0.1 M HCl and O.1 M NaOH. The final pH values were measured and compared to the initial pH values after 24 h of equilibrium time. The pH_{PZC} was calculated by linear interpolation between two neighboring data points whose linear connections intersected with the bisector. The experiment was done in duplicate.

Design of experiments (DoE)

The influence of angle of inclination (θ), influent flow rate (Q) and adsorbate initial concentration (C_i) on Cd^{2+} removal from aqueous solution using IPS-CAC was studied by Box–Behnken Design (BBD) of the Response Surface Methodology (RSM). RSM is a collection of

Table 1 Levels of independent variables and experimental range for Cd^{2+} IPS-CAC experiments

Factor	Variables	Units	Levels of the coded variables		
			−1	0	+1
A	Angle of inclination (θ_p)	°	45	60	75
B	Influent flow rate (Q)	ml/min	5	12.5	20
C	Initial ion concentration (C_i)	mg/l	1	3	5

mathematical and statistical tools used for designing experiments, modeling processes, analyzing independent variables and their interactions, and determining the best parameter values to obtain desired results (Kaur et al. 2021). Equation 2 was used to code the independent variables. In comparison with other RSM techniques, such as central composite design (CCD), BBD requires fewer runs. Most importantly, it avoids analyzing extreme combinations, such as the highest and lowest levels, which could lead to unsatisfactory results.

$$X_i = \frac{X_I - X_0}{\Delta X} \tag{2}$$

where X_i denotes the dimensionless coded value of the of ith variable, X_0 stands for the central variable value and ΔX indicate the change in step. Parameters were coded with three (3) levels: + 1, 0, and − 1, representing the high, center, and low levels, respectively. The independent parameters levels were based on values obtained from various literature as well as prior pilot experimentation are presented in Table 1. The levels of the variable determined based on pretrial laboratory experiment.

The empirical second-order polynomial model (Khedmati et al. 2017) was used for fitting the experimental data. The model terms are represented by Eq. 3.

$$Y = b_0 + \sum b_i X_i + \sum b_{ii} X_i^2 + \sum b_{ij} X_i X_j \tag{3}$$

Y corresponds to the variable response (Cd^{2+} removal). The coefficients b_0 to b_{ij} are constant values where by b_0 is the intercept, b_i is the linear term, b_{ii} is the quadratic term, and b_{ij} is the interactive term. X_i to X_j are the independent variables (such as Angle of inclination, Influent flow rate and Initial ion concentration) as shown in Table 1. A series of 15 experiments including three replications at the central points were conducted in a continuous adsorption setup for Cd^{2+} removal.

Cadmium IPS-CAC continuous experiments and removal efficiency

The Standard 100 mg per liter of Cd^{2+} solution was prepared using the established protocol outlined in the APHA, (2005) standard procedure. The required concentrations for each experiment of the IPS-CAC were attained by progressively diluting the original stock solution (varying from 1 to 5 mg/L). A pH meter (Eutech instruments PH 700 series) was used to measure and adjust the influent's pH to 8.5 before and during the IPS-CAC experimentation. The laboratory scale IPS system comprised of 3 mm thickness Plexiglass fabricated IPS, a peristaltic pump, and the CAC coated settler plates (Fig. 1). The design considerations in the IPS-CAC system design are given as supplementary files (Table S1).

For all the 15-IPS-CAC optimization experimentation, the peristatic pump continuously transferred influent of different concentration from the feed tank through the inlet to the IPS tank with varying plate inclination angles (θ_p) at a controlled rate (Q). The influent from the inlet flow into the bottom of the IPS, raising steadily through the CAC coated plates and was finally discharged at the overflow weir through the outlet into the effluent tank. The section and the 3D isometric view of the IPS-CAC system drawn using AutoCAD 2022 Version 24.1 (AC1032) are shown in Figs. 2 and 3, respectively.

Inductively Coupled Plasma–Optical Emission Spectrometry (ICP-OES) (Agilent 5800) was employed to quantify

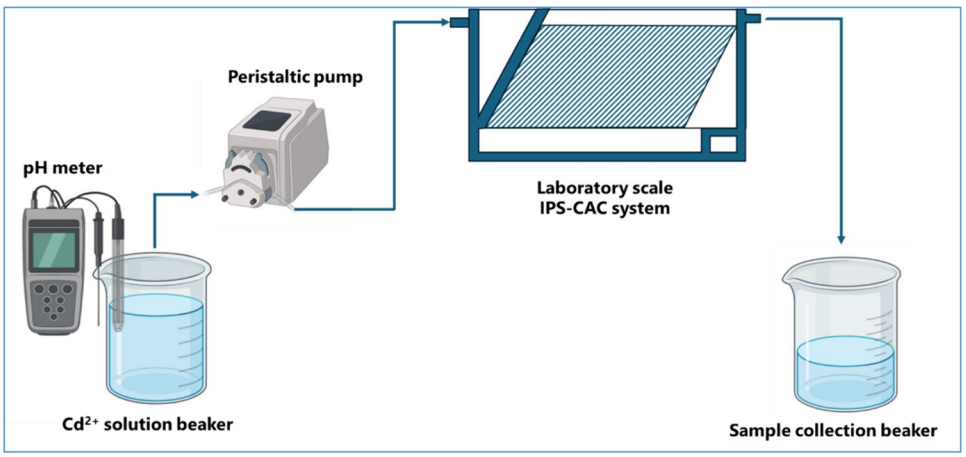

Fig. 1 Schematic diagram of laboratory scale IPS-CAC experimental setup

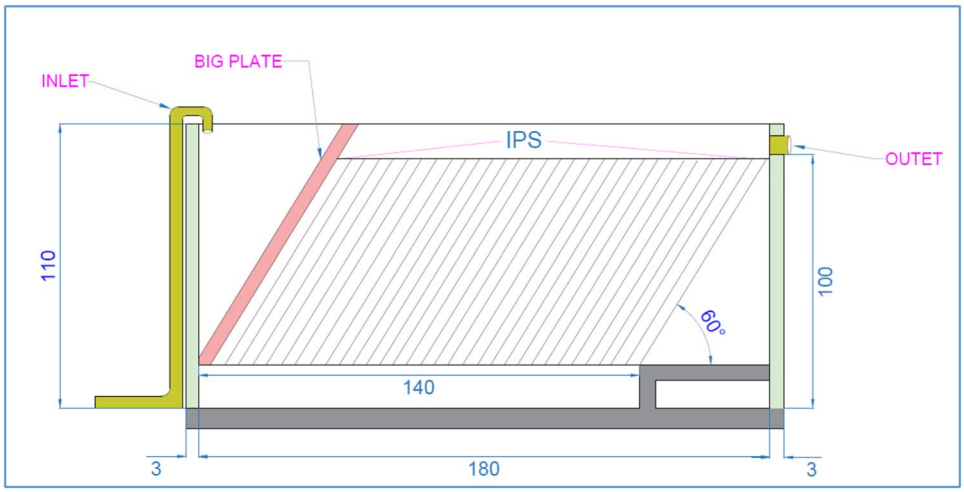

Fig. 2 Section view of the 60° angle inclined plate settler

the concentration of adsorbate before and after adsorption experiment, respectively. Equation 4 was used in calculating the IPS-CAC Cd^{2+} removal efficiency (%).

$$E = \frac{C_i - C_t}{C_i} \times 100 \tag{4}$$

whereas E denotes Cd^{2+} removal efficiency (%), C_i is the initial Cd^{2+} concentration (mg L^{-1}), and C_t denotes the final Cd^{2+} concentration (in mg L^{-1}).

Breakthrough curve analysis and comparative experiments

One goal of continuous or semi-continuous adsorption experiments is to produce a breakthrough curve and compute the maximum solid-phase concentration, which represents the adsorbent's maximal adsorption capacity. Breakthrough curves show how the pollutant concentration in the wastewater changes over time, mainly in a column experimental setup. They can be used to figure out how the continuous sorption process works. The findings may be utilized to develop and operate a full-scale treatment system. After optimization of the operating parameters in the IPS-CAC system, breakthrough experiments were conducted at the optimized conditions for a 14-day (336 h) period.

The width and shape of the mass transfer zone are determined by the adsorption isotherm, flow rate, mass transfer rate to the particles, and diffusion in the pores (Fernandez et al. 2023). Equation 5 can be used to estimate the stoichiometric/breakthrough time.

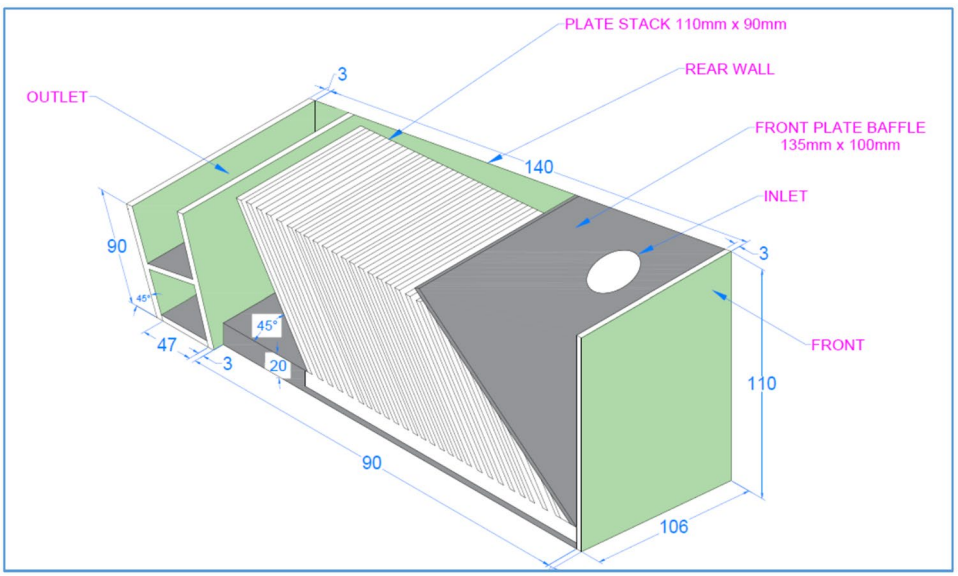

Fig. 3 3D isometric view of the 45° angle inclined plate settler

$$t_b = \int_0^{\infty} \left(1 + \frac{C_b}{C_o}\right) dt \tag{5}$$

where C_b, is the breakthrough concentration (mg/L), C_o is the influent concentration and t_b is the breakthrough time (hrs.).

Equation 5 for breakthrough time or any time t, which represents the area above the curve between the limit t = 0 to t = t, can be written as Eq. 6:

$$t_{st} = \int_0^{t} \left(1 + \frac{C_{st}}{C_o}\right) dt \tag{6}$$

where t_{st} is the saturation time (hrs.) and C_{st} is the saturation concentration at time t_{st}.

Using the breakthrough curve analysis results, the IPS-CAC system overall breakthrough adsorption capacity, *Qe*, (mg/g) of the CAC is calculated using Eqs. 7 and 8.

$$Qe = \frac{(F * C * t * D)}{m} \tag{7}$$

$$D = \left(\frac{C}{C_o}\right)_{final} - \left(\frac{C}{C_o}\right)_{initial} \tag{8}$$

where *Qe* denotes the IPS-CAC overall breakthrough Cd^{2+} adsorption capacity (in mg/g), *F* denotes the optimized influent flow rate (in L/min), *C* and C_o are the breakthrough and initial Cd^{2+} concentration (mg L^{-1}), respectively, *t* is the breakthrough time (in hours) *D* is the C/C_o displacement and *m* denotes the total mass of the CAC adsorbent dosage (in grams). Using Eq. 7, the *t* was replaced with, t_{ex}, exhaustion time (in hours) and similarly the *C* was replaced with C_{ex}, the exhaustion concentration (in mg L^{-1}), to calculate the IPS-CAC adsorption capacity at exhaustion/saturation (in mg/g). In addition, breakthrough curves were obtained by dynamic testing conducted in an IPS-CAC system, where the plate inclination angle, flow rates, and initial influent concentration were each varied at a time; while, the other factors were kept constant. The experiments were carried out at same pH, same total adsorbent dosage and same pump running time corresponding to same total volume of adsorbate per experiment except only for those experiments with varying flow rates. The total mass of adsorbent on CAC was always 45.5 g with a total pump running time of 336 h and adsorbate pH of 8.5. The IPS-CAC removal efficiency at the optimized conditions was also compared with the removal efficiency of a tank with no plates (IPS-NP) and IPS with plain plates (IPS-PP).

Desorption and regeneration potential of CAC

The assessment of adsorption–desorption equilibrium is a key criterion for evaluating the full utilization of all active sites on an adsorbent (Ray et al. 2020; Aktar 2021). Hence, after the assessment of the IPS-CAC Cd^{2+} removal efficiency (%) and overall CAC adsorption capacity (mg/g) under continuous setup, the feasibility of reutilizing the adsorbent was as well examined using a batch adsorption configuration. Batch adsorption–desorption experiments were conducted with 5.34 mg/L adsorbate of pH of 8.5 and 70 mL of 0.1 M HCL of pH 0.3 as the eluent. Spent CAC was each placed in 70 mL desorption liquid in 250 mL flasks, which were subsequently agitated at 20 °C and 200 rpm for 120 min. The adsorption–desorption studies were conducted in triplicates. The regenerated CAC was subjected to three cycles of application in order to analyze its adsorption behavior (Saini et al. 2019). After that, the supernatant was analyzed using ICP-OES to detect the Cd^{2+} concentrations in the samples. Equation 9 was used to calculate the Cd^{2+} quantity that was desorbed (Q_{de}):

$$Q_{de}(mg/g) = \frac{C_i \times V}{W_i} \tag{9}$$

where Q_{de} is the Cd^{2+} desorbed amount (mg/g), *V* is the HCL volume as desorption liquid (*L*), C_i denotes the concentration of Cd^{2+} in the desorption supernatant (mg/L), and W_i is the CAC mass (g). On the other hand, Cd^{2+} desorbed percentage (%) is calculated using Eq. 10:

$$Cd^{2+}desorption(\%) = \frac{Cd_{\ desorbed}}{Cd_{adsorbed}} \times 100 \tag{10}$$

where $Cd_{desorption}$ and $Cd_{adsorption}$ are the concentrations of desorbed and adsorbed Cd^{2+}, respectively.

Model fitting and statistical analysis

Regression analysis and ANOVA were performed on the experimental data using Design-Expert version 11 software. The regression analysis aimed at determining the relationship between the process variables and the Cd^{2+} removal as well as prediction of response variable for new sets of input variables. The main objective of analysis of variance (ANOVA) is to assess whether the independent variables (Angle of Plate Inclination, Flow Rate and Initial Concentration), either individually or in combination, have an impact on the dependent variables (Cd^{2+} Removal Efficiency). The interactions between factors and their effect on the IPS-CAC removal of Cd^{2+} were elucidated by the utilization of the same software program, which also facilitated the development of response surfaces as three-dimensional curves and

two-dimensional contour plots. A measure of the amount of variation around the mean explained by the model was assessed using the R-square (R^2). For comparing the source's mean square to the residual mean square and determine model significant terms F and p values (95% confidence level) were used, respectively. Microsoft Excel (Microsoft Office 2016) and OriginPro (Student Version 2023) were used for calculating the mean 24-h effluent concentration and for plotting graphs, respectively. The breakthrough data was analyzed in Excel and breakthrough graphs were also plotted in the OriginPro software.

Results and discussion

CAC characterization

SEM, BET and FTIR analysis

The results of these physio-chemical properties have been previously reported in Chintokoma, Chebude, Kassahun, et al., (2024). Briefly the CAC SEM illustrates the porous, rough surface resulting from the coated adsorbent, consequently increasing the adsorbent capacity as compared with the plain CCF and the BET surface area (S_{BET}) of the prepared CAC was determined to be 10.6 m^2g^{-1}. The FTIR analysis shows C–H, C=O, and O–H stretching which confirms the presence of a carboxylic acid and not an alcohol (Smith 2011). Following the process of adsorption, the CAC exhibits a nearly complete elimination of the peak heights observed in the FTIR spectrum. The decrease in peak strength seen in the FTIR spectra after Cd^{2+} adsorption indicates the complete participation of functional groups in the adsorption process. Furthermore, the absence of the peaks indicates a prominent and specific adsorption of Cd^{2+} onto the surface of the CAC. The reduction in the intensities of the functional groups on the CAC may be attributed to the bonding of Cd^{2+} with functional groups through the process of oxidation–reduction (Singh et al. 2023).

pH_{PZC} determination

The surface characteristic of the CAC in this investigation was assessed using the Point of Zero Charge (pH_{PZC}), which indicates the pH value at which the surface of the adsorbent becomes electrically neutral (Deng et al. 2009). As shown in Fig. 4, the pH_{PZC} of the prepared CAC is slightly acidic (i.e., a pH_{PZC} of 6). It was crucial to understand the adsorbent's point of zero charge, because it affects the electrostatic interactions occurring between the adsorbate and CAC hence affecting the choice of the experimental pH. For instance, negatively charged adsorbent surface foster electrostatic interactions that facilitate the adsorption of positively charged ions, such as Cd^{2+}, when the solution pH is higher than pH_{PZC}. However, as the pH of the solution drops, the positively charged adsorbent surface facilitates the adsorption of negatively charged ions (Renu et al. 2023). The observed CAC point of zero charge also justifies the pH of the influent that was used in the IPS-CAC optimization experiments.

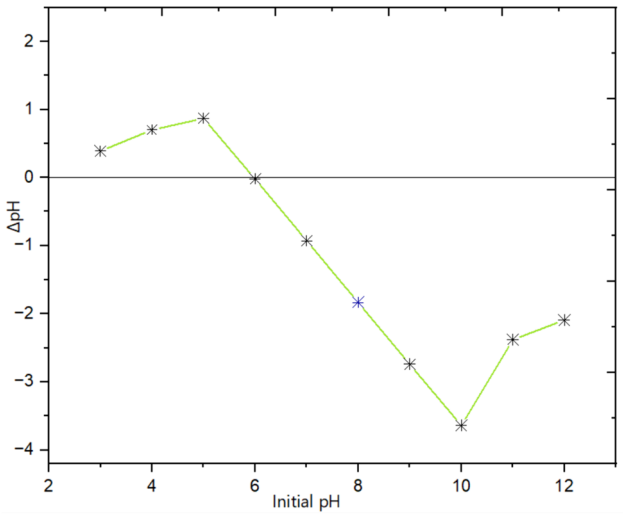

Fig. 4 pH_{PZC} of the prepared 0.25 g dosage CAC

Evaluation of the IPS-CAC Cd^{2+} removal data

Regression model development and validation

The efficacy of a sedimentation tank relies on the physical characteristics of solids and water, as well as the flow and geometric features of the tank (Sarkar et al. 2007). The variables influencing IPS efficiency are tank volume (v_p), plate length (l_p), plate surface area (A_p), plate inclination angle (θ_p), distance between plates (ω_p), number of plates (η_p), roughness of plates (ε_p), density of the particle (ρ_s), density of the water (ρ_w), size of particle (d_s), flow rate (Q), kinematic viscosity water (v_w), initial pollutant concentration (c_i), acceleration due to gravity (g) (Sarkar et al. 2007). Similarly for adsorption, operating parameters like pH, adsorbent dosage, contact time, initial pollutant concentration, temperature and their interactions affect contaminants removal efficiency from aqueous solutions (Amrutha et al. 2023). For this research, all other factors but plate inclination angle of (θ_p), flow velocity (Q), and initial pollutant concentration (c_i) (Table 1) were kept constant. Accordingly, continuous IPS-CAC experiments were performed to study the combined effect of both geometric (angle of plate inclination) and operating factors (flow rate and initial pollutant concentration) on the removal of Cd^{2+} from aqueous media using composite adsorbent coating immobilized on

Table 2 BBD showing actual Cd^{2+} percent removal for IPS-CAC at different operating conditions

Std.	Run	Angle of plate inclination (θ_p)	Flow rate (Q) (ml/min)	Initial concentration (c_i) (mg/L)	IPS-CAC Cd^{2+} removal efficiency (%)
7	1	45	12.5	5	14.8
13	2	60	12.5	3	45.7
1	3	45	5	3	50
6	4	75	12.5	1	35.4
4	5	75	20	3	56.5
15	6	60	12.5	3	42.3
12	7	60	20	5	25
5	8	45	12.5	1	36.3
8	9	75	12.5	5	9.5
14	10	60	12.5	3	39.5
10	11	60	20	1	46.8
2	12	75	5	3	30.4
3	13	45	20	3	23.7
9	14	60	5	1	62.5
11	15	60	5	5	35.1

a substrate in an inclined plate settler. The actual values of the process variables and their variation limits were selected based on data from preliminary studies and various literature sources.

Cd^{2+} removal efficiency is calculated using Eq. 4. Table 2 presents the experimental findings, which shows the actual Cd^{2+} reduction by the IPS-CAC System under different combinations of operating conditions, i.e., angle of plate inclination, flow rate and influent concentration.

The actual and coded second-order polynomial equations describing the IPS-CAC Cd^{2+} removal efficiencies are given by Eqs. 11 and 12, respectively:

$$\begin{aligned}&\text{Actual } Cd^{2+} \text{ removal } \%\\&= 83.17 + 1.97A + -15.83B + 11.39C + 0.17AB\\&\quad + -0.04AC + 0.09BC + -0.03A^2 + 0.19B^2 + -2.73C^2\end{aligned} \tag{11}$$

$$\begin{aligned}&\text{Coded } Cd^{2+} \text{ removal } \%\\&= 42.52 + -1.91A + -6.04B + -12.08C + 18.66AB\\&\quad + -1.1AC + 1.4BC + -7.61A^2 + 10.79B^2 + -10.94C^2\end{aligned} \tag{12}$$

where A = angle of plate Inclination (°), B = flow Rate (ml/min), C = influent concentration (mg/L).

Table 3 presents the p values and F values for assessing the validity of the model prediction for IPS-CAC Cd^{2+} removal efficiency.

The model used for the IPS-CAC removal of Cd^{2+} shows significant high F-value of 74.37 and a low p-value of ≤ 0.0001. This observation suggests that there is a notable influence on the response variable from at least one of the factors included in the model (Brereton 2019). Flow rate and influent concentration were identified as highly significant to the model, all showing low p values ($p < 0.05$) (Table 3). As shown in Table 3, the interaction of angle of plate inclination and flow rate (AB) was also all found to be significant ($p < 0.0001$) for Cd^{2+} removal. Meanwhile, the square terms of all terms (A^2, B^2, and C^2) were all highly significant ($p < 0.0001$) to the Cd^{2+}removal. The obtained lack of fit F-value of 0.099 for Cd^{2+} removal indicated that the lack of fit is not significant to the model.

The model's comparatively high regression coefficient (R^2) of 0.9926 indicate the model's capability of accurately predicting the response. The model has also demonstrated an adequate precision of 31.01, which indicate appropriateness and adequacy to navigate the design space. There is also a good agreement between predicted R^2 (0.9700) and adjusted R^2 (0.9792) as their difference (0.0092) is clearly less than 0.2. The factors added to modify the model have improved the model because the adjusted R^2 is more than the predicted R^2. Hence, the response surface model developed in this research for predicting both Cd^{2+} removal efficiency from aqueous media using IPS-CAC can be considered satisfactory.

Figure 5a shows the normal percentage probability of residual against the normal plot of residuals for Cd^{2+} removal. The figure has a nearly sigmoidal pattern and forms a somewhat linear trend, indicating a strong correlation between probability and normal reduction. This confirms the assumption that the model is appropriate for estimating the efficiency of Cd^{2+} removal.

In contrast, Fig. 5b displays the predicted and actual plots, which corroborate the correlation between the

Table 3 Regression analysis and ANOVA results for quadratic model response surface for Cd^{2+} by IPS-CAC

Source	Sum of squares	df	Mean square	*F*-value	*p*-value	
Model	2932.10	9	325.79	74.37	< 0.0001	Significant
A-Angle of Inclination (θ_p)	25.42	1	25.42	5.80	0.0610	Not significant
B-Flow rate (Q)	234.13	1	234.13	53.45	0.0008	Significant
C-Influent concentration (c_i)	1166.88	1	1166.88	266.38	< 0.0001	Significant
AB	1088.93	1	1088.93	248.58	< 0.0001	Significant
AC	4.80	1	4.80	1.10	0.3431	Not significant
BC	7.84	1	7.84	1.79	0.2386	Not significant
A^2	1162.53	1	1162.53	265.38	< 0.0001	Significant
B^2	400.10	1	400.10	91.33	0.0002	Significant
C^2	385.31	1	385.31	87.96	0.0002	Significant
Residual	21.90	5	4.38			
Lack of fit	2.84	3	0.9451	0.0991	0.9534	Not significant
Pure error	19.07	2	9.53			
Cor total	2954.00	14				

$R^2 = 0.9926$; adjusted $R^2 = 0.9762$; predicted $R^2 = 0.9700$; adequate precision = 31.0084

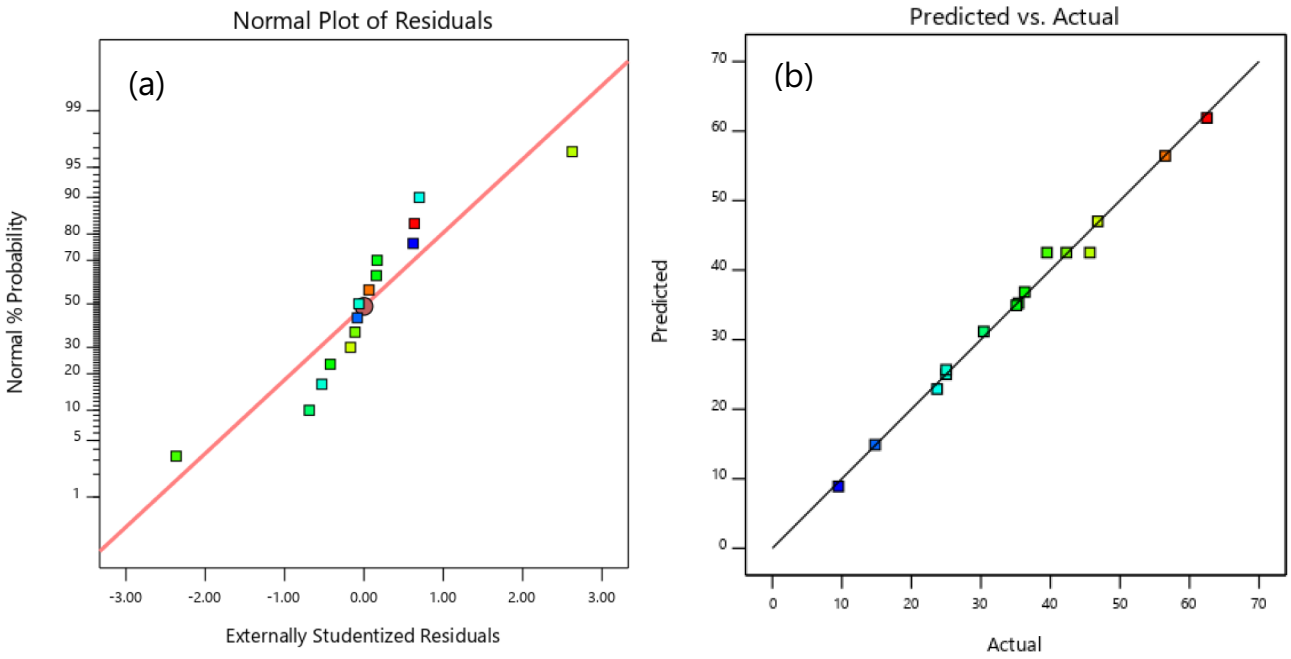

Fig. 5 Normal probability plots (**a**) and plots for predicted against actual results (**b**) for Cd^{2+} reduction by IPS-CAC

residual and expected Cd^{2+} removal. This implies that the model is capable of accurately predicting outcomes within the specified range of both the geometric factor and the operational parameters. Therefore, it can be concluded that the quadratic model of the response surface, which was established in this work to describe the relationship between the Cd^{2+} reduction and geometric factors and the operational parameters, is the most appropriate for accurately representing the experimental results of the innovative IPS-CAC system. In contrast to the conventional "one-parameter-at-a-time approach," which is widely accepted, the use of RSM allows us to understand the individual and interaction effects of the selected operating conditions more effectively. This method enables us to obtain a maximum amount of complex information in a minimal amount of experimental time.

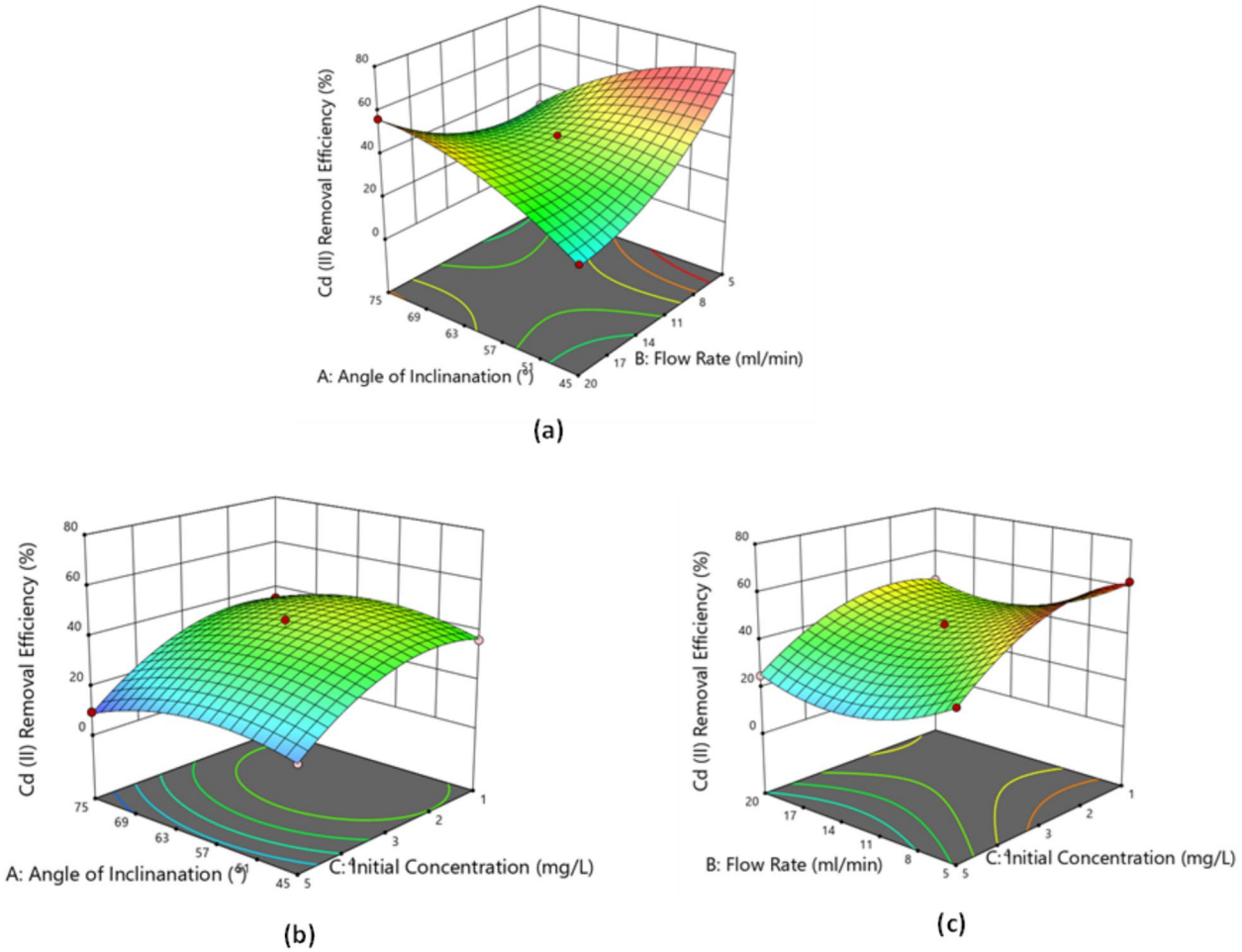

Fig. 6 3D surface response graphs of experimental data showing interacting effect of IPS-CAC operating and geometric factors on Cd^{2+}reduction

Combined influence of geometric and operating conditions on IPS-CAC Cd^{2+} removal efficiency

Three-dimensional (3D) curves represent mathematical functions or parametric equations in three-dimensional space. They allow us to visualize how a curve evolves as we vary one or more independent variables. On the other hand, contour plots are a way to visualize three-dimensional data on a two-dimensional plane. In the present study, the 3D surface response graphs of experimental data showing interacting effect of IPS-CAC geometric and operating factors on Cd^{2+}reduction is shown in Fig. 6. Out of the three combinations of geometric and process factors investigated for their influence on Cd^{2+} removal using RSM, only one interaction between the angle of plate inclination and flow rate (AB) was determined to be significant ($p < 0.0001$), as already presented in Table 3 and discussed above.

Figure 6a shows that Cd^{2+} removal efficiency increases with reducing both plate inclination angle of (θ_p) and flow velocity (Q). The effect of flow rate to the IPS-CAC system could be two- fold. First it relates to the CAC (adsorption) and secondly it relates to the IPS system. At low flow rates, the adsorbate had longer residence time in the IPS unit thereby increasing adsorbate-adsorbent contact time; hence, a high Cd^{2+} removal was achieved. Conversely, high flow rates reduce the residence or the contact time between the adsorbate and adsorbent which lead to insufficient removal of pollutants (Geleta et al. 2021). With increased angle of inclination, the adsorbate-adsorbent contact may further be minimal as the influent can move freely up the plates without contacting the CAC on the IPS plates. Furthermore, an increase in flow rate and an increase in angle of inclination may result in the occurrence of short circuiting in the influent/adsorbate particle flow, causing an uneven distribution of the flow to the plate bundle (Chintokoma et al. 2015). Consequently, this would lead to a particular/affected CAC getting saturated faster than the rest hence allowing adsorbate to leave the treatment chamber up the collecting weir

hence the low removal efficiencies at higher flow rates. Prior research has also indicated that the hydraulic performance of IPS decreases as the flow rate increases (Salem et al. 2011).

Table 3 and Fig. 6b, c show that there is insignificant interacting effect of initial Cd^{2+} concentration (c_i) and inclination angle of (θ_p) (Fig. 6b) and that of initial Cd^{2+} concentration (c_i) and flow velocity (Q) (Fig. 6c) on Cd^{2+} removal by IPS-CAC system. Nevertheless, Fig. 6b, c indicate that the IPS-CAC Cd^{2+} removal efficiency decreases with an increase in initial Cd^{2+} concentration at any given plate inclination angle or flow rate, respectively. At low concentrations, metals are absorbed by specific sites. However, as the metal concentrations increase, the specific sites become saturated and the exchange sites are filled (Mouni et al. 2012). The adsorption capacity of a given amount of adsorbent is constant, allowing for the adsorption of a finite quantity of heavy metal ions. As the initial concentration rises, the levels of heavy metal ions likewise progressively rise. The heavy metal ions will gradually occupy the surface adsorption sites and reach a state of saturation. The adsorption capacity of the adsorbent for heavy metal ions rises per unit and eventually achieves an equilibrium condition. Hence, given a certain adsorbent quality, higher initial concentrations result in decreased removal efficiency of heavy metal ions (Li et al. 2022).

In reference to the findings as explained above, when an inclined plate settler (IPS) is coated with a composite adsorbent, the settling and adsorption processes work together to remove Cd^{2+} more efficiently. The inclined plates increase the contact time and surface area for the wastewater to interact with the adsorbent; while, composite adsorbent materials provide a higher capacity for cadmium capture. This synergistic effect results in a more effective removal process than either component could achieve alone.

Process optimization

The main objective of the optimization method was to determine the most favorable values of variables for effectively removing Cd^{2+} utilizing the IPS-CAC hybrid. This was accomplished by employing a model generated from empirical data. The operating parameters were selected with the aim of maximizing the response (i.e., Cd^{2+} removal efficiency); while, the angle of inclination, flow rate and influent concentration were all left at a range. Multiple sets of experiments (42 in total) were suggested by the model but the one with high removal efficiency was selected for further verification as well as breakthrough curve and comparative studies. The optimized operating conditions (i.e., angle of inclination, $\theta = 45°$; Flow rate, $Q = 5$ ml/min and influent concentration, $C_i = 1.87$ mg/L) predicted 75.8% removal for Cd^{2+} with 0.76 desirability. Experimentally, the same optimum operating conditions were able to achieve $66.9 \pm 0.48\%$ Cd^{2+} removal efficiencies.

Breakthrough analysis study

The primary motivation for this study is the need to develop a scalable prototype for wastewater treatment. In this context, the use of mathematical modeling is crucial for the successful implementation of upscaling methods. It facilitates the transfer of knowledge from laboratory studies to pilot plants and industrial scales. The mathematical modeling serves as a powerful tool for analyzing and interpreting experimental data, identifying key processes, predicting outcomes under various operating conditions, and enhancing the overall efficiency of the treatment process (de Franco et al. 2017). Breakthrough occurs when the adsorbate reaches the end of the system and exits with the system effluent (Gabelman 2017). The breakthrough curves were obtained from the continuous 336-h IPS-CAC experimental results at the optimized conditions. The graph illustrating the relationship between adsorbate concentration and time is displayed in Fig. 7 which show the breakthrough curves for the sorption of Cd^{2+} on the immobilized CAC. The quantity of adsorbate adsorbed at a specific moment is exactly proportional to the surface area located above the breakthrough curve at that moment bounded by $C_t/C_o = 1$ (Gabelman 2017); where C_t is the Cd^{2+} effluent concentration at time t, C_o is the initial of influent concentration. Where t_b is the breakthrough time, breakthrough was achieved when $C_t/C_o = 0.25$. C_{ex} and t_{ex} are the exhaustion/saturation concentration and time, respectively, when $C_t/C_0 = 0.95$, i.e., a point at which 95% of the CAC was exhausted. Hence exhaustion time (t_{ex}) was taken at exhaustion concentration C_{ex} when C_t/C_o attained a value of 0.95. The breakthrough data was effectively utilized to determine the adsorption capacity at both breakthrough (t_b) ($C_t/C_0 = 0.25$) and exhaustion (t_{ex}) ($C_t/C_0 = 0.95$) times. Figure 7b shows that the breakthrough and saturation times were 66.9 and 168.15 h, respectively. Using Eq. 7, the IPS-CAC overall breakthrough adsorption capacity (q_b) was determined to be 6.17 mg/g; while, the IPS-CAC adsorption capacity at exhaustion (q_{ex}) was calculated as 15.51 mg/g. Experimentally, the optimized conditions yielded 74.3% removal at zero hours of first effluent and an average Cd^{2+} removal efficiency of 69.7% over a 96-h period.

Adsorption dynamics

Figure 8 shows the breakthrough curves of Cd^{2+} adsorption onto IPS-CAC at different plate inclination angles, initial Cd^{2+} concentrations and flow rates. Breakthrough time, is defined as the time required to reach a specific breakthrough outlet concentration (Dorado et al. 2014). As mentioned already, the breakthrough time was reached when C_t/C_o

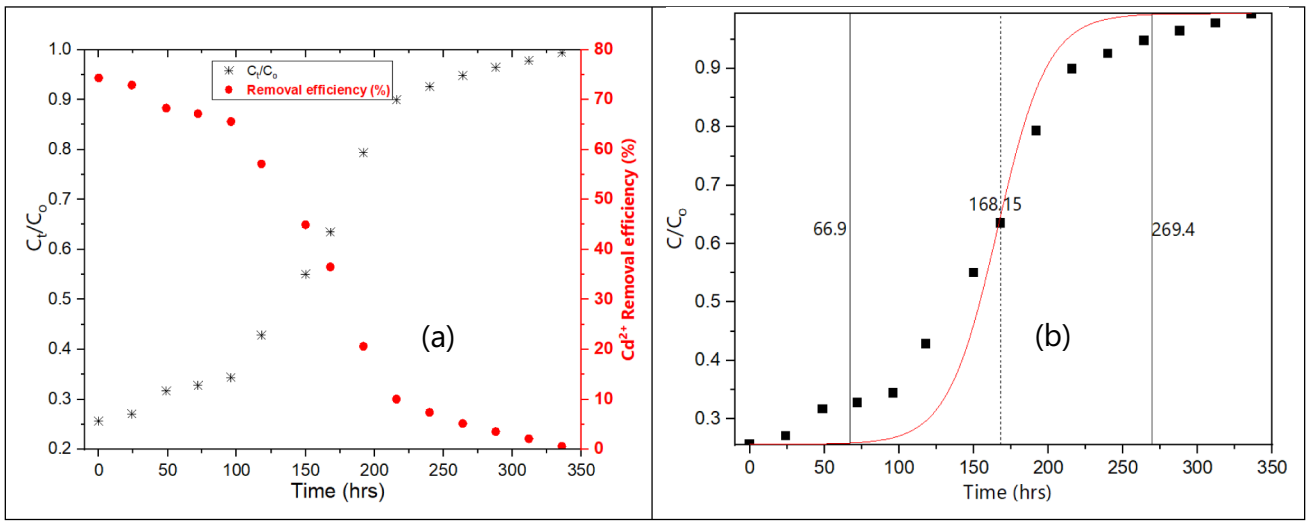

Fig. 7 Optimized conditions breakthrough experimental results (**a**) and breakthrough curve analysis (**b**) of the IPS-CAC system

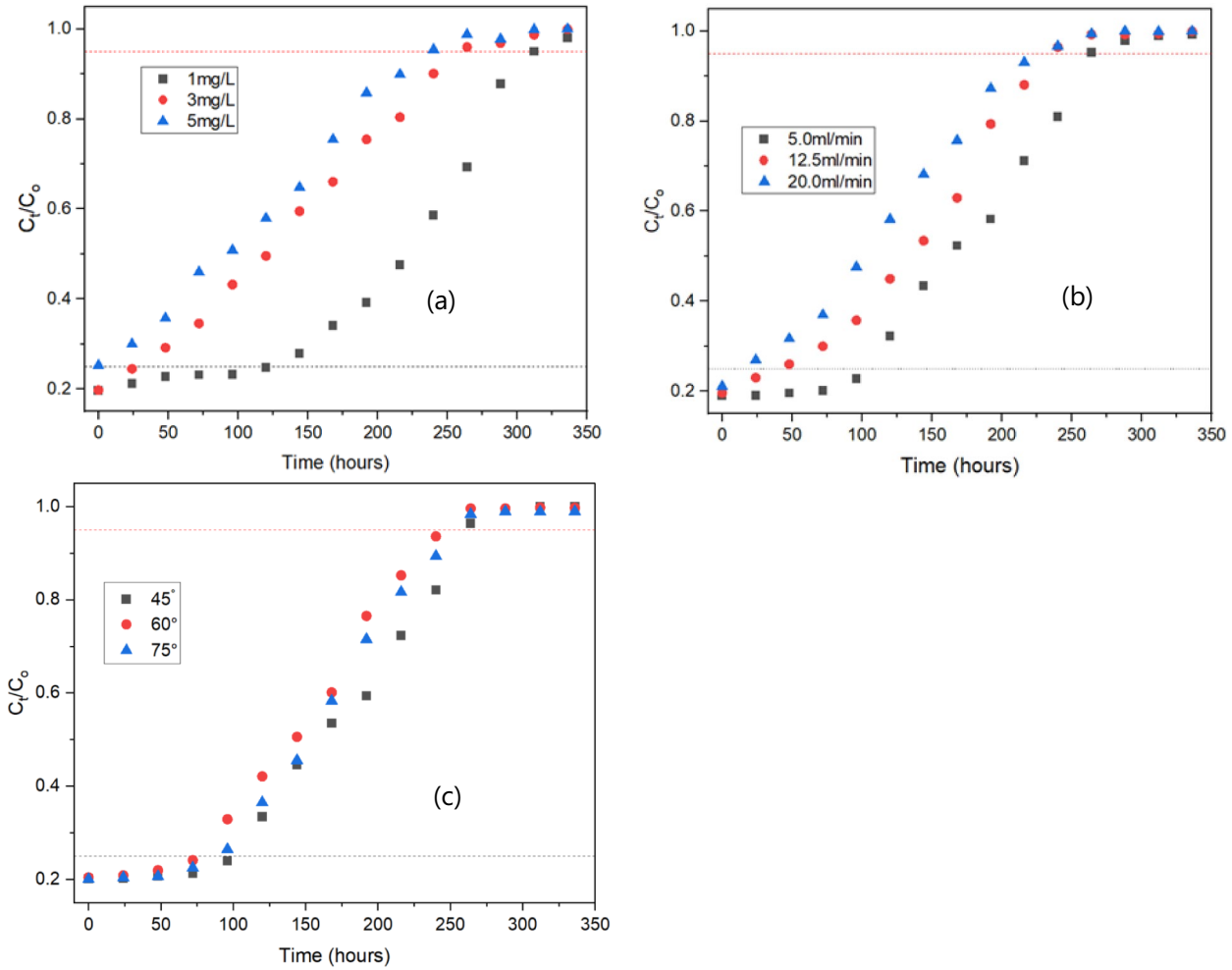

Fig. 8 Breakthrough curves of Cd^{2+} onto IPS-CAC at different conditions (**a**) Varying initial $Cd.^{2+}$ concentration ($\theta = 45°$ and $Q = 5$ ml/min), (**b**) Varying flow rate ($\theta = 45°$ and $C_o = 1$ mg/L) and (**c**) Varying plate inclination angle ($C_o = 1$ mg/L and $Q = 5$ ml/min)

was equal to 0.25. Similarly, saturation or exhaustion time was reached at $C_t/C_o = 0.95$. The total IPS-CAC adsorption capacities at both breakthrough and saturation point were obtained by numerical integration of the area above the breakthrough curve up to $C_t/C_o = 1$ (Gómez-Avilés et al. 2022).

Figure 8a shows that the breakthrough time increases with decreasing initial Cd^{2+} concentration meaning that lower metal concentrations generates higher adsorption zone lengths (Dorado et al. 2014) there by increasing the adsorption capacity. Furthermore, it was observed that the gradient of the breakthrough curves got steeper when the initial Cd^{2+} concentration was increased. Previous studies have attributed this to the reaction zone progressing more rapidly under higher metal concentrations (Antil et al. 2022; Dorado et al. 2014). Approximately 120 h were required to obtain the breakthrough point for the lowest 1 mg/L influent compared to the 23.6 h and 3 h that was needed to reach the breakthrough point for both the 3 mg/L and 5 mg/L influent, respectively. The breakthrough adsorption capacities at different Cd^{2+} concentrations of 1, 3 and 5 mg/L were 5.93, 3.5 and 0.74 mg/g, respectively. The decline in adsorption capacity with increasing concentration observed at the breakthrough point is attributed to the saturation of adsorption sites on the CAC. Consequently, the adsorbent's surface reached saturation more rapidly at higher concentrations (Patel 2020) leading to relatively lower adsorption capacity.

The effect of Cd^{2+} removal by IPS-CAC on varying flow rates were studied at 5, 12.5, and 20 ml/min; while, initial influent concentration and plate inclination angle were kept constant at 1.89 mg/L and 45°, respectively. Both the breakthrough time and adsorption capacity decreased with an increase in flow rate (Fig. 8b). The breakthrough time were 118, 36, and 15.5 h corresponding to breakthrough adsorption capacities of 5.84, 4.45, and 3.07 mg/g for the 5, 12.5 and 20 ml/min flow rates, respectively. High flow rate reduces the residence time and contact time between the adsorbate and adsorbent leading to reduced breakthrough time relatively adsorption capacities (Geleta et al. 2021; Ledesma et al. 2023; Mondal et al. 2018). The observed variations in the adsorption capacity and the breakthrough curve's steepness with varying flow rates may be explained by the basic principles of mass transfer (Tosun 2019). Higher flow rates minimize the resistance to mass transfer caused by external coating at the adsorbent's surface, resulting in a faster rate of mass transfer and a decreased residence time (Fernandez et al. 2023).

Finally, it can be seen from Fig. 8c how the breakthrough time does not vary significantly with the angle of plate inclination. This observation agrees well with the results of the ANOVA results of the optimization experiments in Table 3 showing the insignificant ($p = 0.05$) effect of IPC-CAC plate inclination angle on Cd^{2+} removal. The breakthrough time of the 45°, 60° and 60° IPS were 100, 80 and 60 h respectively corresponding to adsorption capacities of 4.95, 3.96 and 2.97 mg/g, respectively.

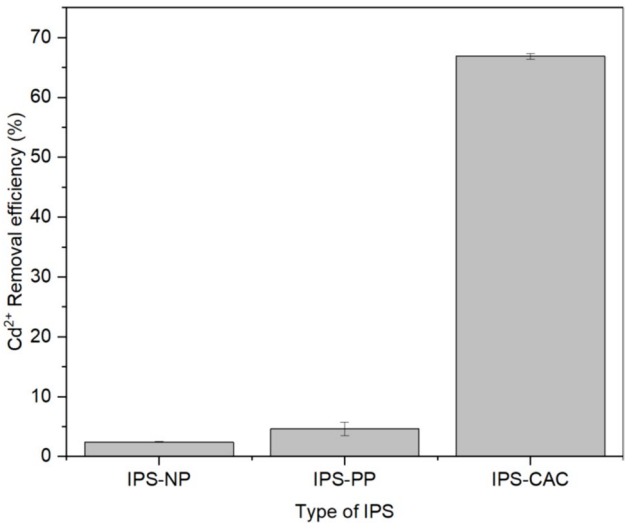

Fig. 9 Optimized conditions breakthrough curve analysis results of the IPS-CAC system

3.7 Comparative experiments

After optimization of the IPS-CAC geometric and process factors, the IPS-CAC removal efficiency at the optimized conditions was also compared with the removal efficiencies of IPS with plain plates (IPS-PP) and a tank with no plates (IPS-NP). Figure 9 presents results of the comparison of the percentage removal of Cd^{2+} by IPS-CAC, IPS-NP and IPS-PP, respectively. Vividly, there is a significant ($p < 0.05$) difference in removal efficiencies with IPS-CAC having higher removal efficiency (66.9%) compared to IPS-PP (4.6%) and IPS-NP (2.4%). Clearly the comparative experiment results confirm that that the higher IPS-CAC system removal of Cd^{2+} from the wastewater was achieved due to the synergistic effect of IPS and CAC. As explained above, the CA-IPS system not only improve Cd^{2+} removal efficiency but also enhances the scalability for large-scale applications.

CAC regeneration studies and re-usability potential

The efficacy of a particular biomass being as adsorbent depends not only on its adsorption capability, but also on its ease of regeneration and recycling (Younas et al. 2021). The ability of the adsorbent to regenerate and be recycled is another important component of the adsorption process (Aktar 2021). The CAC was mainly synthesized to overcome the challenges associated with leaching of adsorbents during regeneration (Azha et al. 2017; Shamsudin and Shahadat 2019). The Cd^{2+} desorption amount, $\mathcal{Q}_{de}$, (mg/g) and

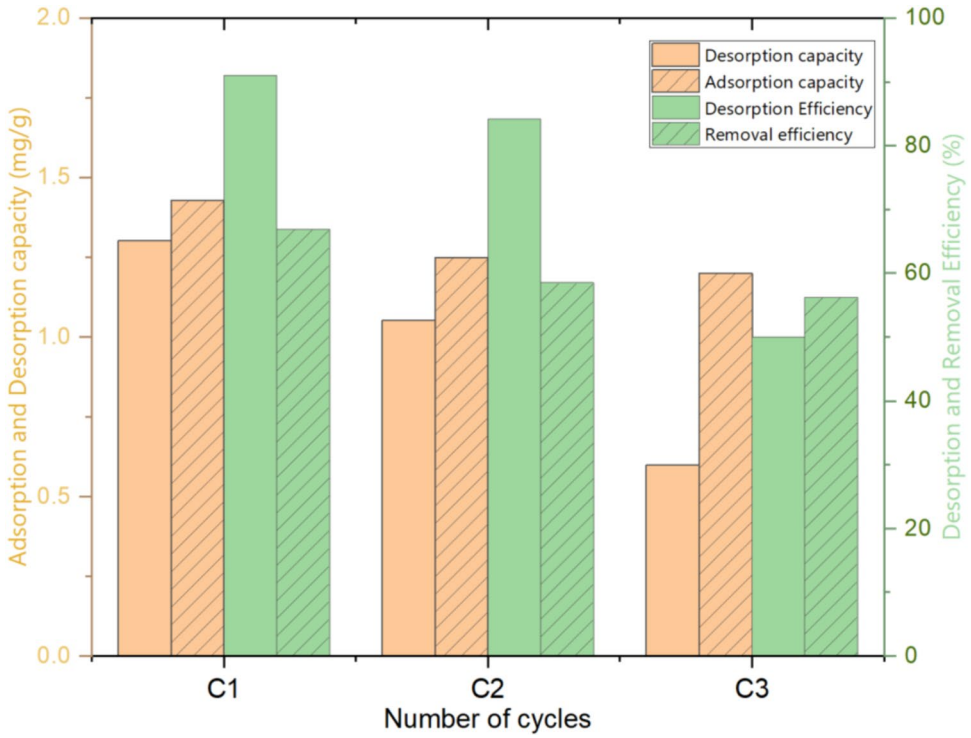

Fig. 10 Cd^{2+} adsorption and desorption capacity of HCL from CAC surface and its Cd^{2+} adsorptive and desorption removal efficiency of regenerated CAC

desorption percentage (%) of CAC calculated using Eqs. 9 and 10, respectively. Figure 10 show that the adsorption capacity of CAC decreased only slightly after each adsorption–regeneration cycle.

The regeneration study shows that the CAC lost just about 10.7% (from 66.9 to 56.2%) of its Cd^{2+} removal efficiency with HCL as an eluent even after three consecutive adsorption–desorption tests. On the other hand, the desorption percentage (%) reduced from 91 to 50% following three successive cycles. This demonstrates the great stability of the CAC and its potential for three consecutive cycles of Cd^{2+} adsorption–desorption. However since the CCF used in making the CAC is basically cotton fiber composed of cellulose, accompanied by a limited number of non-cellulosic components (Kumar et al. 2022), the disintegration of the cotton fibers from the use of HCL as de-sorbent is evident especially after the third cycle of regeneration.

Conclusion

The IPS-CAC system was developed, fabricated, and optimized as a scalable prototype for wastewater treatment, specifically for removing heavy metals. The goal was to enhance the efficiency of heavy metal removal by leveraging the combined effect of IPS and CAC. To study the impact of plate inclination angle (θ), influent flow rate (Q), and initial adsorbate concentration (C_i) on the removal efficiency of Cd^{2+}, the Box–Behnken Design (BBD) of the Response Surface Methodology (RSM) was employed. The results indicated that flow rate and initial influent concentration were the most significant factors ($p < 0.05$) affecting Cd^{2+}removal by the IPS-CAC system. Furthermore, the interaction between plate inclination angle (θ) and flow rate (Q) had a significant contribution to the reduction of Cd^{2+} ($p < 0.05$). The optimal conditions for Cd^{2+} removal was achieved with a plate inclination angle (θ) of 45°, a flow rate (Q) of 5 ml/min, and an influent concentration (C_i) of 1.87 mg/L. By using these optimized parameters, the IPS-CAC system was predicted to achieve a Cd^{2+} removal efficiency of 75.8%. Experimental results at these optimized conditions showed an average removal efficiency of 69.7% over a 96-h period through the synergistic effects of IPS-CAC. The breakthrough time ($C_t/C_o = 0.25$) and saturation time ($C_t/C_o = 0.95$) under the optimized conditions were determined to be 66.9 h and 168.2 h, respectively, with adsorption capacities of 6.17 mg/g and 15.51 mg/g at breakthrough and saturation points, respectively. The CAC demonstrated a high stability in Cd^{2+} removal, with only a 10% decrease (from 69.7 to 59.7%) in efficiency observed after three adsorption–regeneration cycles. This observation indicates that the composite material can be effectively reused to remove Cd^{2+} ions from effluent streams. The CAC's ability to eliminate the need for filtration, sedimentation, or centrifugation during regeneration makes it an attractive option for scalable and practical industrial applications.

Additionally, the IPS-CAC system is easily scalable, reducing the footprint of the treatment unit and operating in a gravity-operated manner, thereby minimizing initial and operational costs, as well as the carbon footprint. In general, this study was conducted in lab-scale experimental setup of which ideally was supposed to be under controlled environments, however due to unavailability of appropriate experimental materials some parameters were not easily controlled. For future work, it would also be essential to conduct a pilot scale experimentation of the IPS-CAC design in order to have a comprehensive understanding of system performance.

Supplementary Information The online version contains supplementary material available at https://doi.org/10.1007/s13201-024-02292-2.

Acknowledgements The authors express their sincere gratitude to the staff at both the Department of Separation Science at LUT University, Finland, and the Institute of Catalysis and Petrochemistry (ICP) of the Spanish National Research Council (CSIC), Spain, for their invaluable support in conducting SEM analysis and isotherm experiments for estimating BET surface area, respectively. The authors are also grateful to Jurgen van der Linden of the Mallard Creek Polymers (MCP) for facilitating the supply of the Acrylic Polymer Emulsion (APE) that was used in this research.

Author contributions GCC contributed to conceptualization, methodology, investigation, formal analysis, and writing—original draft preparation. YC contributed to supervision, writing—review & editing, resources. SKK contributed to supervision, formal analysis, writing—review and editing. AD contributed to resources, writing—review & editing. TK contributed to resources.

Funding The author(s) received no specific funding for this work.

Declarations

Conflict of interest The authors declare that they have no known competing financial interests or personal relationships that could have appeared to influence the work reported in this article.

Compliance with ethical standards The research did not involve any procedures involving human participants, hence did not require any ethical approvals.

References

Aktar J (2021) Batch adsorption process in water treatment. In: Intelligent environmental data monitoring for pollution management. Elsevier Inc. https://doi.org/10.1016/b978-0-12-819671-7.00001-4

American Public Health Association (2005) Standard methods for the examination of water and wastewater. In: American Public Health Association (APHA): Washington, DC, USA.

Amrutha Jeppu G, Girish CR, Prabhu B, Mayer K (2023) Multi-component Adsorption Isotherms: Review and Modeling Studies. In: Environmental processes, Vol. 10, Issue 2. Springer International Publishing. https://doi.org/10.1007/s40710-023-00631-0

Antil M, Singh S, Bhagat M, Vilvas V, Sundaramurthy S (2022) Column optimization of adsorption and evaluation of bed parameters-based on removal of arsenite ion using rice husk. Environ Sci Pollut Res 29(48):72279–72293. https://doi.org/10.1007/s11356-022-20580-9

Azha SF, Shahadat M, Ismail S (2017) Acrylic polymer emulsion supported bentonite clay coating for the analysis of industrial dye. Dyes Pigm 145:550–560. https://doi.org/10.1016/j.dyepig.2017.05.009

Azha SF, Ismail S (2019) Immobilization of dye pollutants on composite adsorbent coating: Screening, efficiency and adsorption mechanism. In: AIP conference proceedings, 2124(July). https://doi.org/10.1063/1.5117131

Bo S, Tao C, Xuxuan C, Guo Y, Shenghao Z (2015) Effect of inclined plate dissolved air gas float processing on oilfield wastewater. J Petrochem Univ 28(5):6–10

Brereton RG (2019) ANOVA tables and statistical significance of models. J Chemom 33(3):1–5. https://doi.org/10.1002/cem.3019

Chintokoma GC, Chebude Y, Kassahun SK (2024) Cd2+ removal efficiency of activated carbon from Prosopis juliflora: optimization of preparation parameters by the Box–Behnken Design of Response Surface Methodology. Heliyon 10(10):e31357. https://doi.org/10.1016/j.heliyon.2024.e31357

Chintokoma GC, Chebude Y, Kassahun SK, Demesa AG, Koiranen T (2024) Sol-gel synthesis of composite adsorbent coating from Prosopis juliflora –activated carbon for simultaneous adsorptive removal of Cd^{2+} and Cr_2O_7 CrOfrom wastewater. AQUA Water Infrastruct Ecosyst Soc 73(5):945–968. https://doi.org/10.2166/aqua.2024.335

Chintokoma GC, Machunda RL, Njau KN (2015) Optimization of Sedimentation Tank Coupled with Inclined Plate Settlers as a Pre-treatment for High Turbidity Water. 5(17), 11–24.

Clark SE, Elligson JC, Bradley Mikula J, Roenning CD, Siu CYS, Hafera JM (2007a) Inclined plate settlers to treat stormwater solids. In: Restoring our natural habitat - proceedings of the 2007 world environmental and water resources congress, August, 621–626. https://doi.org/10.1061/40927(243)580

Clark SE, Elligson JC, Bradley Mikula J, Roenning CD, Siu CYS, Hafera JM (2007b) Inclined plate settlers to treat stormwater solids. In: Restoring our natural habitat - proceedings of the 2007 world environmental and water resources congress. https://doi.org/10.1061/40927(243)580

de Franco MAE, de Carvalho CB, Bonetto MM, de Pelegrini Soares R, Féris LA (2017) Removal of amoxicillin from water by adsorption onto activated carbon in batch process and fixed bed column: kinetics, isotherms, experimental design and breakthrough curves modelling. J Clean Product 161:947–956. https://doi.org/10.1016/j.jclepro.2017.05.197

Demim S, Drouiche N, Aouabed A, Benayad T, Dendene-Badache O, Semsari S (2013) Cadmium and nickel: assessment of the physiological effects and heavy metal removal using a response surface

approach by L. gibba. Ecol Eng 61:426–435. https://doi.org/10.1016/j.ecoleng.2013.10.016

Deng H, Yang L, Tao G, Dai J (2009) Preparation and characterization of activated carbon from cotton stalk by microwave assisted chemical activation-Application in methylene blue adsorption from aqueous solution. J Hazard Mater 166(2–3):1514–1521. https://doi.org/10.1016/j.jhazmat.2008.12.080

Dorado AD, Gamisans X, Valderrama C, Solé M, Lao C (2014) Cr(III) removal from aqueous solutions: a straightforward model approaching of the adsorption in a fixed-bed column. J Environ Sci Health - Part A Toxic/hazardous Substan Environ Eng 49(2):179–186. https://doi.org/10.1080/10934529.2013.838855

Dorea CC, Williams JG, Boulay-Côté F, Bédard G, Bouchard C (2014) Sustainable water and sanitation services for all in a fast changing world inclined plate settling for emergency water treatment: towards optimisation. In: 37th WEDC International Conference, Hanoi, Vietnam, 2014, 0–4. https://repository.lboro.ac.uk/articles/conference_contribution/Inclined_plate_settling_for_emergency_water_treatment_towards_optimisation/9595811

Elligson JC, Mikula JB, Clark SE, Roenning CD, Hafera JM, Franklin KA (2014) Inclined plate settlers to treat stormwater solids. Proc Water Environ Fed 2006(6):5609–5623. https://doi.org/10.2175/193864706783775711

Fernandez RMD, Estrada RJR, Tomon TRB, Dingcong RG, Amparado RF, Capangpangan RY, Malaluan RM, Dumancas GG, Lubguban AA, Alguno AC, Bacosa HP, Lubguban AA (2023) Experimental design and breakthrough curve modeling of fixed-bed columns utilizing a novel 3D coconut-based polyurethane-activated carbon composite adsorbent for lead sequestration. Sustainability (Switzerland) 15(19):14344. https://doi.org/10.3390/su151914344

Filipič M (2012) Mechanisms of cadmium induced genomic instability. Mutat Res – Fundam Mol Mech Mutagenesis 733(1–2):69–77. https://doi.org/10.1016/j.mrfmmm.2011.09.002

Gabelman A (2017) Adsorption basics: Part 1. Chem Eng Progr 113(8):1–6

Geleta WS, Alemayehu E, Lennartz B (2021) Enhanced defluoridation of water using zirconium—coated pumice in fixed-bed adsorption columns. pp 1–20

Genchi G, Sinicropi MS, Lauria G, Carocci A, Catalano A (2020) The effects of cadmium toxicity. Int J Environ Res Public Health 17(11):1–24. https://doi.org/10.3390/ijerph17113782

Gómez-Avilés A, Peñas-Garzón M, Belver C, Rodriguez JJ, Bedia J (2022) Equilibrium, kinetics and breakthrough curves of acetaminophen adsorption onto activated carbons from microwave-assisted $FeCl_3$-activation of lignin. Sep Purif Technol 278(January):119654. https://doi.org/10.1016/j.seppur.2021.119654

Gul A, Ma'amor A, Khaligh NG, Julkapli NM (2022) Recent advancements in the applications of activated carbon for the heavy metals and dyes removal. Chem Eng Res Design 186:276–299

Gupta A, Sharma V, Sharma K, Kumar V, Choudhary S, Mankotia P, Kumar B, Mishra H, Moulick A, Ekielski A, Mishra PK (2021) A review of adsorbents for heavy metal decontamination: growing approach to wastewater treatment. Materials 14(16):1–45. https://doi.org/10.3390/ma14164702

Hu J, Chen J, Liu F, An S, Shi Y, Luan Z, Xiao J, Zhang B (2022) Enhancing oil removal from wastewater by combining inclined plate settler and electrocoagulation. Sep Sci Technol (Philadelphia) 57(17):2824–2835. https://doi.org/10.1080/01496395.2021.1993258

Hyun K, Kang Y (2023) Performance of inclined-plate settler and activated carbon sponge-cube media filter for the treatment of urban stormwater runoff from an industrial complexs. KSCE J Civ Eng 27(9):3686–3693. https://doi.org/10.1007/s12205-023-2307-y

Kasenene AJ, Machunda RL, Njau KN (2021) Performance of inclined plates settler integrated with constructed wetland for high turbidity water treatment. Water Pract Technol 16(2):516–529. https://doi.org/10.2166/wpt.2021.009

Kaur G, Singh N, Rajor A (2021) RSM-CCD optimized Prosopis juliflora activated carbon for the Adsorptive uptake of Ofloxacin and disposal studies. Environ Technol Innov 25:102176. https://doi.org/10.1016/j.eti.2021.102176

Kayhanian M, Murphy K, Regenmorter L, Haller R (2001) Characteristics of storm-water runoff from highway construction sites in California. Transp Res Rec 1743:33–40. https://doi.org/10.3141/1743-05

Khedmati M, Khodaii A, Haghshenas HF (2017) A study on moisture susceptibility of stone matrix warm mix asphalt. Constr Build Mater 144:42–49. https://doi.org/10.1016/j.conbuildmat.2017.03.121

Kumar P, Sai Ram C, Srivastava JP, Behura AK, Kumar A (2022) Synthesis of Cotton Fiber and Its Structure. Nat Synthetic Fiber Reinforced Compos. https://doi.org/10.1002/9783527832996.ch2

Ledesma B, Sabio E, González-García CM, Román S, Fernandez ME, Bonelli P, Cukierman AL (2023) Batch and continuous column adsorption of p-nitrophenol onto activated carbons with different particle sizes. Processes 11(7):1–22. https://doi.org/10.3390/pr11072045

Leung WF, Probsteln RF (1983) Lamella and tube settlers. 1. Model and operation. Ind Eng Chem Process Design Dev 22(1):58–67. https://doi.org/10.1021/i200020a011

Li J, Dong X, Liu X, Xu X, Duan W, Park J, Gao L, Lu Y (2022) Comparative study on the adsorption characteristics of heavy metal ions by activated carbon and selected natural adsorbents. MDPI. https://www.mdpi.com/2071-1050/14/23/15579

Mahdi RK, Naji NM, Al-Mamoori SOH, Al-Rifaie ZI, Ali RN (2021) Effect cadmium on living organisms. IOP Conf Ser Earth Environ Sci. https://doi.org/10.1088/1755-1315/735/1/012035

Mondal P, Mehta D, Saharan VK, George S (2018) Continuous column studies for water defluoridation using synthesized magnesium-incorporated hydroxyapatite pellets: experimental and modeling studies. Environ Process 5(2):261–285. https://doi.org/10.1007/s40710-018-0287-6

Mouni L, Merabet D, Bouzaza K, Belkhiri L (2012) Removal of Pb^{2+} and Zn^{2+} from the aqueous solutions by activated carbon prepared from Dates stone Removal of Pb^{2+} and Zn^{2+} from the aqueous solutions by activated carbon prepared from Dates stone. *Desalination and Water Treatment*, *June 2014*. https://doi.org/10.5004/dwt.2010.1106

Patel H (2020) Batch and continuous fixed bed adsorption of heavy metals removal using activated charcoal from neem (Azadirachta indica) leaf powder. Sci Rep 10(1):1–12. https://doi.org/10.1038/s41598-020-72583-6

Ray SS, Gusain R, Kumar N (2020) Effect of reaction parameters on the adsorption. Carbon Nanomaterial-Based Adsorbents for Water Purification, 119–135. https://doi.org/10.1016/b978-0-12-821959-1.00006-4

Renu MA, Singh K (2023) Simultaneous removal of heavy metals and dye from wastewater: modelling and experimental study. Water Sci Technol 87(1):193–217. https://doi.org/10.2166/wst.2022.410

Saini S, Katnoria JK, Kaur I (2019) A comparative study for removal of cadmium(II) ions using unmodified and NTA-modified *Dendrocalamus strictus* charcoal powder. J Environ Health Sci Eng 17(1):259–272. https://doi.org/10.1007/s40201-019-00345-2

Salem AI, Okoth G, Tho J (2011) An approach to improve the separation of solid e liquid suspensions in inclined plate settlers: CFD simulation and experimental validation. Water Res 5:1–9. https://doi.org/10.1016/j.watres.2011.04.019

Sarkar S, Kamilya D, Mal BC (2007) Effect of geometric and process variables on the performance of inclined plate settlers in treating

aquacultural waste. Water Res 41(5):993–1000. https://doi.org/10.1016/j.watres.2006.12.015

Shamsudin MS, Shahadat M (2019) Cellulose/bentonite-zeolite composite adsorbent material coating for treatment of N-based antiseptic cationic dye from water. J Water Process Eng 29(August):100764. https://doi.org/10.1016/j.jwpe.2019.02.004

Singh V, Pant N, Sharma RK, Padalia D, Rawat PS, Goswami R, Singh P, Kumar A, Bhandari P, Tabish A, Deifalla AM (2023) Adsorption Studies of Pb(II) and Cd(II) Heavy Metal Ions from Aqueous Solutions Using a Magnetic Biochar Composite Material. Separations 10(7):389. https://doi.org/10.3390/separations10070389

Smith BC (2011) Fundamentals of FTIR. https://ds.amu.edu.et/xmlui/bitstream/handle/123456789/7157/%5BBrian_C._Smith%5D_Fundamentals_of_Fourier_Transform%28BookZZ.org%29.pdf?sequence=1&isAllowed=y

Somma S, Reverchon E, Baldino L (2021) Water purification of classical and emerging organic pollutants: an extensive review. ChemEngineering 5(3):47. https://doi.org/10.3390/chemengineering5030047

Tosun I (2019) Fundamental mass transfer concepts in engineering applications. In: Fundamental mass transfer concepts in engineering applications. Taylor & Francis Group. https://doi.org/10.1201/b22432

Wisniewski E (2014) Sedimentation tank design for rural communities in the hilly regions of Nepal. J Humanitarian Eng 2(1):43–54. https://doi.org/10.36479/jhe.v2i1.15

Younas F, Mustafa A, Ur Z, Farooqi R, Wang X, Younas S, Mohyud-din W, Hameed MA, Abrar MM, Maitlo AA, Noreen S, Hussain MM (2021) Current and emerging adsorbent technologies for wastewater treatment: trends, limitations, and environmental implications. Water 13(215):1–25

Zhang H, Zheng S, Zhang X, Duan S, Li S (2020) Optimizing the inclined plate settler for a high-rate microaerobic activated sludge process for domestic wastewater treatment: a theoretical model and experimental validation. Int Biodeterior Biodegradation 154(May):105060. https://doi.org/10.1016/j.ibiod.2020.105060